Effect of Side Wall Expansion Angle on the Performance of a Dump Diffuser Model for a Combustor

T. B. V. Chetan[†] and S. Chakrabarti

Department of Mechanical Engineering, Indian Institute of Engineering Science and Technology, Shibpur, Howrah-711103, West Bengal, India

†*Corresponding Author Email: chetanteki@gmail.com*

ABSTRACT

In the present article, numerical analysis has been performed on a dump diffuser model, to study the effect of sidewall expansion angle (SWA), on its performance aspects. SWA has been varied from 90° to 1° and performance has been evaluated in terms of major influencing aspects. It is observed that, at SWA of magnitudes greater than 11°, there is no significant change in the performance. But at SWA below 11°, significant changes, which enhance the performance are observed. It is noticed that at SWA in range, from 3.57° to 8°, higher static pressure recovery (almost from 25 to 33% of inlet dynamic pressure) happens in the dump and annular regions. SWA of magnitudes less than 11° have resulted in smaller, low dense and higher intense recirculation zones. At the SWA of 3.57°, static pressure recovered is maximum and total pressure lost is minimum. But that SWA causes too much delay in pressure stabilization on the liner wall. However, SWA of magnitudes less than 3.57° have resulted in comparatively poor performance. Eventually, sidewall angle in the range from 5° to 7° is found to be optimum as it yields higher static pressure recovery and low total pressure loss. This range also results in early stabilization of pressure both on the liner and casing walls.

Keywords: Sidewall Angle; Corner recirculation zone; Converging and diverging area; Static pressure recovery; Total pressure loss.

NOMENCLATURE

AR	area ratio	θ_{PD}	pre-diffuser Angle (degrees)
C_P	static pressure recovery coefficient (dimensionless)	θ_{SW}	sidewall Angle (degrees)
D_G	dump gap	ε	turbulent energy dissipation rate
D_L	liner diameter	μ	dynamic viscosity
D_C	casing diameter	ν	kinematic viscosity
h_1	inlet diameter	ρ	fluid density
h_2	outlet diameter	λ	total pressure loss coefficient (dimensionless)
k	turbulent kinetic energy		
L	inlet length		
L_{PRE}	pre-diffuser length (m)	Subscripts	
L_S	settling length	i, j	denotes the indices of tensorial notation
L_V	vertical sidewall length	1	represents any parameter at inlet section
$\dot{m}$	mass flow rate	2	represents any parameter at outlet section
P	static pressure		
P_t	total pressure	Superscripts	
U	inlet Mean velocity	*	denotes non-dimensional quantities
V	mean velocity at any location	‾	denotes mass-weighted mean value
x, y	cartesian coordinates		
$P_{D\text{-}IN}$	inlet dynamic pressure		

1. INTRODUCTION

In gas turbine engines, air from compressor approaches combustor at speeds of range 130-170m/s. At those conditions, flow Mach number is less than 0.33, this allows the flow to be considered as an incompressible flow. However, at such high speeds, maintaining a stable flame is practically impossible. So, a diffuser is installed next to the compressor exit, in order to decelerate the flow to lower speeds and ensure stable and efficient combustion. During the flow through a diffuser, static pressure rises and total pressure losses considerably. So, an efficient diffuser must cause minimum total pressure loss along with higher static pressure rise. Figure 1 represents the two commercially used diffusers. Fig 1 (a) represents the faired diffuser and Fig. 1 (b) represents the dump diffuser. Figure 1 is considered from the work of Fishenden and Stevens (1977). Faired diffuser decelerates the flow by the phenomena of solid wall expansion in three regions, which include annular divergence and central divergence of the flow. Though, the faired diffuser is associated with less loss in total pressure but occupies larger length. It is sensitive to compressor outlet conditions, manufacturing tolerances of the annular area and local thermal distortions due to combustion. Modern high bypass ratio aircraft engines are associated with smaller annular gaps. So, a better alternative for these modern engines is the dump diffuser, which is of shorter lengths and insensitive to all the factors mentioned above. Dump diffuser consists of a pre-diffuser section, where static pressure increases mostly. Then, the fluid is dumped into a region formed between the exit plane of the pre-diffuser and the blunt dome face of the combustor. This region is referred to as the dump region. As the flow expands suddenly, a corner recirculation zone (CRZ) is formed in the dump region. CRZ is referred to as stationary vortex in Fig. 1. Area variation occurring between the free surface of this CRZ and the dome wall is converging and diverging (CDA) in nature. In the diverging region of this CDA variation, the flow undergoes free surface diffusion into the annular region, which is formed between the casing wall and the liner wall. This process allows the dump diffuser, for being insensitive to compressor exit conditions, manufacturing tolerances and thermal distortions in the annular area. The size of the CRZ formed in the dump diffuser includes both the axial and radial extension of it. It is understood that radial and axial extensions of the CRZ are dependent on two flow aspects. The radial extension of the CRZ depends on the nature of geometrical area (GA) variation occurring at the pre-diffuser exit. While the axial extension of CRZ is dependent on the nature of CDA variation occurring between the free surface of CRZ and the dome wall. However, during the flow through the annular region, there are primary, secondary and dilution holes along the liner wall. It is through these holes, the fluid discharges into the combustion chamber. Both the total pressure, the static pressure of the fluid along the liner should be higher, to ensure proper

penetration and specified flow through these holes. This affects the combustion reaction and the combustor outlet temperature distribution. As fluid is diffused suddenly into the dump region, the losses associated with dump diffusers are higher than that of faired diffusers. In dump diffusers, the total pressure loss occurs in the pre-diffuser, dump and annular regions. These losses which occur without any reaction and just by the fluid dynamic phenomena are termed as cold losses. While those occurring after the combustion reaction, are the hot losses. It has been experimentally proven and known from the study on literature that, cold losses are much higher than hot losses (Cohen *et al* (2017)). These cold losses contribute a lot to the static and total pressure loss in the combustor. These losses eventually lead to the thrust reduction of the aircraft. This is the reason, because of which much research has been going on non-reacting isothermal flow conditions in a combustor from the last few decades.
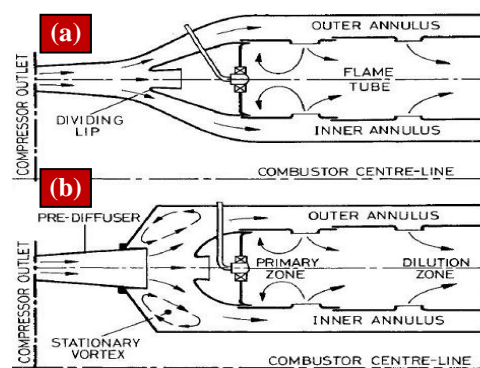
Fig. 1. Diffuser Types Faired Diffuser (b) Dump Diffuser (Fishenden and Stevens (1977)).

Dump diffuser has been considered for the study because of its relative advantages over the faired diffuser. One of which is being independent to the inlet velocity profile. The aspect mentioned above has been studied and concluded by Biaglow (1971). He has performed an experimental investigation on two diffuser models, which are a simple wide-angle diffuser and a dump diffuser. He has studied the exit temperature profile for two models, for different inlet velocity profiles. He has finalized that dump diffuser is almost insensitive to the inlet velocity changes. Many works have been carried out on the dump diffuser by considering different geometric and flow parameters. Some of the earlier works that are done on a dump diffuser model include the works done by Fishenden and Stevens (1977) and Koutmos and McGuirk (1989). Fishenden and Stevens (1977) have experimentally studied the effect of dump gap, mass flow split between inner, outer annuli on a simple sudden expansion type dump diffuser. Their main conclusion is that static pressure rises mostly in the pre-diffuser. While most of the total pressure loss occurs in the dump and settling length region. Koutmos and McGuirk (1989) have made a numerical study using finite difference formulation for turbulent isothermal flow in a model, same as Fishenden and Stevens (1977). They have

considered experimental results of Fishenden and Stevens (1977) till the pre-diffuser part and mainly concentrated on the dump and annular regions to study the effect of dump gap and mass flow split. They have noticed that at the dump gap of 1.0, static pressure recovery coefficient (C_P) curve descends with respect to the increase in flow split, after reaching a maximum value. But at a dump gap of 1.5, it remains almost flat with respect to the increase in flow split, after reaching a maximum value. Those conclusions of the above works have initiated the motivation in the authors to increase the static pressure recovery in the dump, annular regions and thereby reduce the total pressure loss in those regions. Conclusions of the above works have also helped the authors to finalize the dump gap that needs to be considered for the present study. Rahim et al. (2002) have carried out an experimental investigation on the effect of dump gap, inlet swirl on the casing and liner wall pressure distribution of a can type combustor model. They have concluded that reattachment length is proportional to dump gap and dump gap has no influence on the liner wall pressure distribution. They have mentioned the important requirements of the liner wall and casing wall pressure distributions. Ghose et al. (2016) have studied numerically, the effect of pre-diffuser angle (PDA) on the liner wall and casing wall pressure variation, with and without inlet swirl. They have considered 4 pre-diffuser angles which are 0°, 12°, 27°, and 50°. Their results conclude that C_P becomes almost constant for PDA in the range between 15° and 18°. The conclusions of the above works have motivated the authors to study the liner and casing wall pressure distributions along with flow field study in the present work. Along with this, the work of Ghose et al. (2016) has given an idea of the range in which PDA for the present work is to be considered. Another geometrical parameter which has a significant effect on the performance of dump diffuser is the dome head shape. Rahim et al. (2007) have performed an experimental study, to find the effect of dome head shape on the performance of a combustor model, with and without inlet swirl. They have considered three dome shapes namely hemispherical, vertical ellipsoidal and horizontal ellipsoidal. Their results have manifested that hemispherical dome shape yields better values of C_P and λ, for the case with no inlet swirl. Ghose et al. (2013) have made a numerical study on the effect of dome shape on liner and casing wall pressure variation. Dome shapes considered by them are the same as Rahim et al. (2002). Their study also yields better results for hemispherical dome shape for the case with no inlet swirl. Conclusions of the above two studies have motivated the authors to consider the hemispherical dome head shape of the present study. Gaurav et al. (2002) have numerically studied the effect of annular height on the performance of a model dump diffuser. Their results conclude that at an annular area ratio of 2.236, uniform velocity and pressure are achieved along the liner wall. They have observed that total pressure loss increases proportionally with annular area ratio. Xu et al. (2015) have performed studies on a model dump diffuser, both numerically and experimentally. They

have compared the results obtained by using different turbulence closure models with experimental results. They have reported that the Reynolds stress model is in better agreement with experimental results. The above-mentioned study has initiated the thought of using the Reynolds stress model for the present work. Further study regarding the turbulence closure model to be used in the present study is discussed in the later sections. Das and Chakrabarti (2015) have numerically analyzed an isothermal laminar flow in a conventional can type combustor. They have studied the effect of Reynolds number, aspect ratio, central restriction area percentage, aspect ratio, and a fence with a fixed angle on the flow field and axial velocity profiles of the combustor. They have observed that CRZ size increases with an increase in Reynolds number, percentage central restriction and aspect ratio. This study has motivated the authors to study the axial velocity profiles at different axial locations in the present work, to get a better understanding of the flow field. Das and Chakrabarti (2016) have numerically analyzed a 2D laminar flow in a dump combustor. They have studied the effect of Reynolds number, aspect ratio, central restriction area percentage along with different magnitudes of suction, at the corner above the throat section, on pressure characteristics of the combustor. They have concluded that the magnitude of static pressure rise after throat section of the combustor increases with increase in Reynolds number, central restriction area percentage. This work has motivated the authors to study the total pressure variation along the liner wall in the present study. Regarding the sidewall angle (SWA), much work has not been done on analyzing its complete effect on the performance of dump diffuser. Sarkar et al. (2004) have made a numerical study of isothermal swirling flow in a conventional can type combustor, by applying the k-ε turbulence closure model. They have studied the effect of sidewall expansion angle on the flow pattern, by varying it from 90° to 30°. They have concluded that, at low swirl levels, flow patterns are almost uninfluenced by the sidewall expansion angle. Rhode et al. (1983) have made experimental as well as numerical analysis on the flow field of the model combustor, at SWA 90°, 45° for different swirl angles along with no inlet swirl. They have found that for non-swirling flows, the effect of SWA on the flow field is negligible. Kumar et al. (2007) have performed a numerical study on two different dump diffuser models, both with 12° pre-diffuser angle. One is a simple sudden expansion model, while the other has SWA of 67.5°. They have studied pressure distribution on liner, casing walls by varying dump gap and turbulent intensity. They haven't noticed any advantage for the inclined sidewall. But they have concluded that low dump gap with high turbulent intensity gives a remarkable improvement in pre-diffuser pressure recovery. Kumar et al. (2007), Rhode et al. (1983) have considered inclining the sidewall as a typical case. So, they have analyzed at a particular SWA and have come up with a conclusion as mentioned above. However, Sarkar et al. (2004) have considered some typical SWA magnitudes such as

90°, 60°, 45°, and 30°. The probable reason behind not considering lower magnitudes of SWA by them may be explained as follows. They have considered only swirling flow analysis on a conventional combustor. In a swirling flow, most of the flow is in the radial and tangential directions. For this type of flow in a can type combustor, provision of lower magnitudes of SWA may reduce the volume of the combustion chamber and also reduces the axial diffusion of the flow. Therefore, they might have analyzed at only higher magnitudes of SWA. It is clear from the above studies that in all the works that are done by considering SWA as a variable, they have only taken specific magnitudes of SWA. But no work has been done till date, to study the effect of SWA by varying it from higher to much lower magnitudes. This has motivated the authors to study the effect of various sidewall angles, from higher to lower magnitudes, on the performance of a non-swirling, 2D turbulent isothermal flow through a dump diffuser and finally come up with a narrow range of SWA which yields optimum performance in terms of required aspects.

2. MATHEMATICAL FORMULATION

2.1. Computational Domain

The computational domain that has been considered for the present study is shown in Fig. 2. The important dimensions of the configuration are taken as follows. Area ratio (AR) (h_2^2/h_1^2) is 1.46. Non-dimensional (ND) entrance length (L/h_1) is 1.85. ND dump gap [D_G/h_2], affects the flow field immensely. If it is too high, static pressure recovered in the pre-diffuser is less. While too less value of it causes higher magnitudes of flow turning, which leads to total pressure loss. From the work of Fishenden and Stevens (1977), it is observed that loss coefficient is minimum, in the dump gap range of from 1.0 to 1.5, for a model with AR=1.4, L/h_1=1.9. Along with the aspects mentioned above, the conclusions of the works of Rahim *et al.* (2002) and Kumar *et al.* (2007) have been considered to finalize the ND dump gap value of 1.16 in the present work. Pre-diffuser angle (PDA) causes much of the static pressure recovery. Too higher values of it lead to flow separation on its wall, as per the results of Ghose *et al.* (2016). At lower magnitudes of PDA such as 12°, 18°, from Klein (1995), it is clear that losses at 18° are higher than those at 12°. The results of Xu *et al.* (2015) also show evidential flow separation on the pre-diffuser wall, for a diffuser with 18° included PDA. Klein *et al.* (1974) has proposed that total pressure loss associated is lower and almost constant, for PDA of magnitudes within 12.5°. Based on all these conclusions, PDA has been considered to be 12°. Moreover, lower PDA is required here, in order to vary SWA to very small magnitudes. Dome shape dictates the flow turning and acceleration during free surface diffusion. Based on the conclusions of Rahim *et al.* (2007) and Ghose *et al.* (2013), hemispherical dome shape has been considered for present work. Other relevant dimensions of the diffuser are taken as, h_1=0.054m, h_2=0.06534m,

L_{PRE}=0.054m, D_L=0.0762m. For proper stabilization of the flow, ND settling length (L_S/h_1) is considered as 6.35. D_C is considered to be 0.1524m, based on the conclusions of Gourav *et al.* (2002) and Klein (1995). Higher values of it allow for sufficient change in the SWA and also results in higher pressures in the annular region. Vertical sidewall length (L_V) is considered as 0.015m, for all the cases except for SWA of magnitudes 1° and 2°. It has been fixed so, in order to vary SWA to much lower magnitudes.
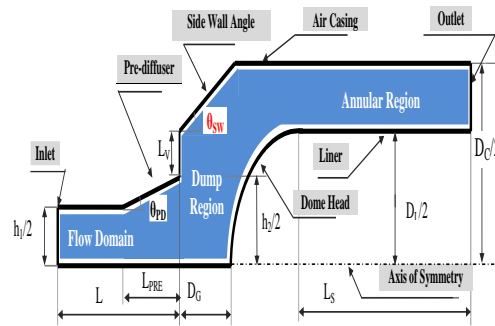
Fig. 2. Computational domain of present study.

In the present study, SWA magnitude has been varied from 90° to 20° at a step of 10° and from 15° to 1° at a step of 1°, for a detailed analysis. SWA 3.57° is the extreme case, where there is a continuous divergence in the flow path until the outlet, as shown in Fig. 5(e). For further lower angles such as 1°and 2°, L_V has been varied accordingly.

2.2. Numerical Methodology

Numerical simulation in the present study is carried out on a 2D model. The reason behind this consideration is as follows. In the present study, the analysis is carried out for non-swirling flow. In a non-swirling flow, there are no gradients of any parameters in the tangential direction and the flow is symmetric about the axis. So, it is appropriate to consider a 2D model for the present analysis. Mesh configuration considered for present 2D analysis is shown in the Fig 3(a), Fig. 3(b), and Fig. 3(c). The considered flow domain has been meshed with a minimum element size of 0.3mm. Inflation has been applied at all the walls, which grows smoothly at a rate of 1.1 for 8 layers. In all cases, the numbers of mesh elements (mesh no.) are considered in the range from 110000 to 140000, based on the mesh independency as shown in Fig. 3(d) and Fig. 3(e). Fig. 3(d) and Fig. 3(e) represent the variation of C_P and λ with respect to mesh no. respectively, for two SWA magnitudes.

Turbulence model that is considered for the closure of the problem is the Reynolds stress model (RSM), with linear pressure strain and standard wall function. Date (2005) has mentioned that eddy viscosity models are weak to predict and RSM is more suitable for predicting strong separating flows, free shear flows and flows involving 2D diffusion. Those phenomena are expected for the flow in domains such as that considered for the present

work. The reason behind this suitability is that, in models like k-ε model, Boussinesq Approximation is considered. This approximation assumes eddy viscosity to be isotropic in nature. But, flow in the considered model exhibits higher anisotropy in the properties.
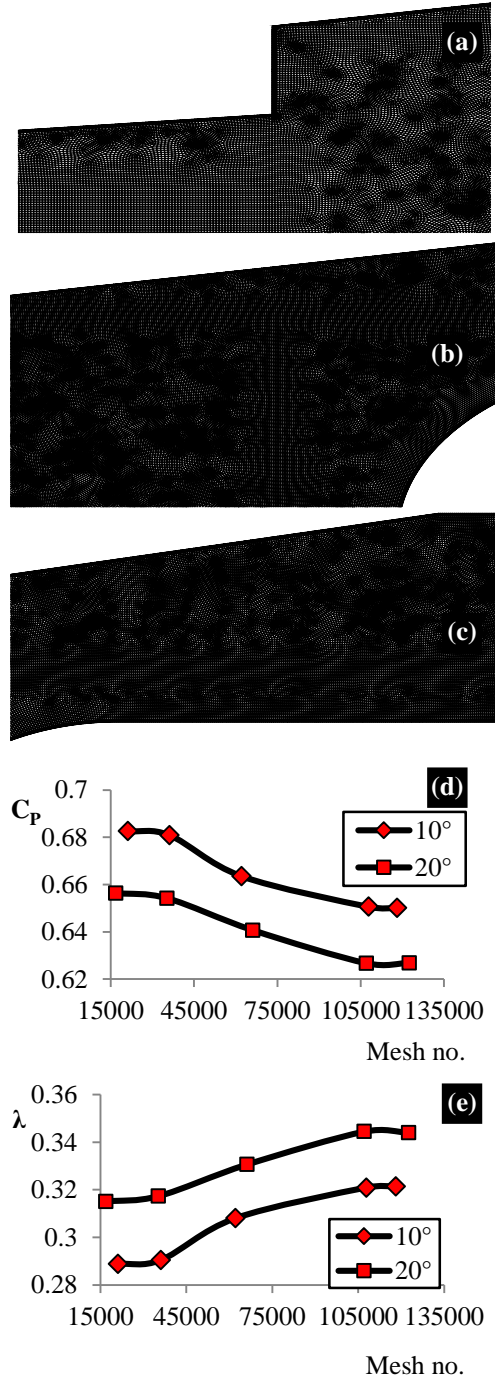
Reynolds stresses separately. So, the concept of isotropic eddy viscosity is avoided. This makes it suitable for the flows in sudden expansion, diverging passages like the flow in considered model. The theoretical aspects mentioned above regarding the RSM are studied from the work of Clarke *et al*. (1989). Even Xu.*et al*. (2015) has reported that the results of RSM are in better agreement with experimental results than other eddy viscosity models. The theoretical benefits of RSM are also been stated in Ganeshan *et al*. (2007). Governing equations considered and solved in RSM are given below. Equation (1) and Eq. (2) are the conservative forms of continuity and Reynolds Averaged Navier Stokes equations respectively. Equation (3) is the conservation equation of the turbulent energy dissipation rate (ε). Equation (4) is the expression for turbulent kinetic energy (k). Equation (5) represents the transport equation of Reynolds stress component.

$$\frac{\partial(\rho V_j)}{\partial x_j} = 0 \tag{1}$$

$$\frac{\partial(\rho V_i V_j)}{\partial x_j} = -\frac{\partial \overline{P}}{\partial x_i} + \frac{\partial}{\partial x_j}\left[\mu \frac{\partial(V_i)}{\partial x_j} - \rho \overline{u_i u_j}\right] \tag{2}$$

$$\frac{\partial(V_k \varepsilon)}{\partial x_k} = C_\varepsilon \frac{\partial}{\partial x_k}\left[\frac{k}{\varepsilon}\overline{u_k u_l}\frac{\partial \varepsilon}{\partial x_l}\right] + \frac{1}{2}C_{\varepsilon 1}\frac{\varepsilon}{k}P_{kk} - C_{\varepsilon 2}\frac{\varepsilon^2}{k} \tag{3}$$

$$k = \frac{1}{2}\overline{u_i u_j} \tag{4}$$

$$\frac{\partial(\rho V_k \overline{u_i u_j})}{\partial x_k} = \rho(P_{ij} - \varepsilon_{ij} + \phi_{ji} + d_{ijk}) \tag{5}$$

$$P_{ij} = -\left[\overline{u_j u_k}\frac{\partial V_i}{\partial x_k} + \overline{u_i u_k}\frac{\partial V_j}{\partial x_k}\right]$$

$$\phi_{ji} = -C_1\frac{\varepsilon}{k}\left[\overline{u_i u_j} - \frac{2}{3}\delta_{ij}k\right] - C_2\left[P_{ij} - \frac{1}{3}\delta_{ij}P_{kk}\right]$$

$$d_{ijk} = C_S\frac{\partial}{\partial x_k}\left[\frac{k}{\varepsilon}\overline{u_k u_l}\frac{\partial \overline{u_i u_j}}{\partial x_l}\right]$$

$$\varepsilon_{ij} = 2\nu\frac{\overline{\partial u_i}}{\partial x_k}\frac{\partial u_j}{\partial x_k} = \frac{2}{3}\delta_{ij}\varepsilon$$

Here, P_{ij} represents the production term of Reynolds stress. φ_{ji} represents the pressure strain term. d_{ijk} represents the diffusion term of Reynolds stress. ε_{ij} is the turbulent dissipation rate. δ_{ij} is the Kronecker delta function. x_i, x_j, x_k are the spatial coordinates in i, j, k directions respectively. u_i, u_j, u_k, u_l are the velocity fluctuations in i, j, k, l directions respectively. V_i, V_j, V_k are the mean velocities in i, j, k directions respectively. Values of constants in the equations are considered as follows. $C_{m\mu} = 0.09, C_{\varepsilon 1} = 1.44, C_{\varepsilon 2} = 1.92, \sigma_k = 1.0, \sigma_\varepsilon = 1.3, C_1 = 1.8, C_2 = 0.6, C_\varepsilon = 0.22, C_s = 0.1$. The above-mentioned equations, along with the values of the constants, are taken from Xia *et al.* (1998).

Fig. 3. Mesh configuration and Mesh independency results (a) Mesh configuration in dump region, (b) Mesh configuration in annular region, (c) Mesh configuration in pre-diffuser region (d) Variation of CP with mesh no. (e) Variation of λ with mesh no.

Ansys Fluent 15.0 software is used to solve the above flow field. For pressure-velocity coupling, the SIMPLE algorithm (Semi-Implicit Method for Pressure-Linked Equations) has been employed with the second order upwind scheme. For

RSM solves the transport equations of individual

convergence criteria, non-dimensional normalized residuals of all parameters are considered to reach 10^{-6}. Air is the fluid considered with properties, density (ρ) =1.225 kg/m³, dynamic viscosity (μ) =1.7894x10^{-5} kg/m-Sec Turbulent intensity =3.708% and turbulent length scale = 0.00378, are calculated based on inlet Reynolds number (Re) using expressions for those parameters from Ghose *et al.* (2013). Inlet velocity for the present analysis is considered to be 32.46 m/s and inlet temperature is taken as 305K. Mach number corresponding to those inlet conditions is 0.1. The Mach number magnitude above which the flow compressibility effect is considered is 0.33. As Mach number in the present case is less than 0.33, this flow is considered to be incompressible.

2.3. Boundary Conditions

The boundary conditions that are applied for the numerical analysis are as follows.

- At the inlet, velocity is considered to be 32.46 m/s. It is considered so, based on the conclusion of Hestermann *et al.* (1991) that in the range of Re from $9.2*10^4$ to $1.6*10^5$, the performance of dump diffuser is almost independent of Re, both at small and large dump gaps. This aspect is also stated in Klein (1995) and Lefebvre *et al.* (2009).

- At the outlet, the pressure is considered to be atmospheric, based on the conclusions of Gaurav *et al.* (2002) and Ganeshan *et al.* (2008).

- Walls are subjected to no-slip condition.

- Axisymmetric condition is applied at the central line.

3. RESULTS AND DISCUSSION

Non-dimensional (ND) forms of different parameters that are used for the manifestation of results are taken as given below.

- ND length: $X^* = x/D_C$, $Y^* = y/D_C$

- ND Static pressure: $P^* = {}^P/_{P_{D-IN}}$

- ND Total Pressure: $P_t{}^* = {}^{P_t}/_{P_{D-IN}}$

- ND velocity: $V^* = V/U$

3.1. Validation of results

The results of the present work are validated with the experimental results of Rahim *et al.* (2002) and Rahim *et al.* (2007). The model considered for validation is the same as that of the above-mentioned works. Static pressure variation along the casing, liner walls is compared with corresponding experimental results of Rahim *et al.* (2002), as shown in Fig. 4(a) and Fig. 4(b) respectively. RMS error calculated based on the data in Fig. 4(a) and Fig. 4(b) is observed to be 2% and 5.28% respectively. For further validation, **C**$_P$, **λ** values of the present study are compared with experimental values of those parameters reported by Rahim *et al.* (2007), as shown in Table 1 From Table 1, it is observed that absolute error in case of

C$_P$ is 8.92% and that for **λ** is 6.9%. Theoretical limitation of the error for judging the accuracy of any predicted result is considered to be 10%. Error in case of both the above-mentioned comparisons is less than 10%. This ensures that present numerical study is in good agreement with experimental studies.
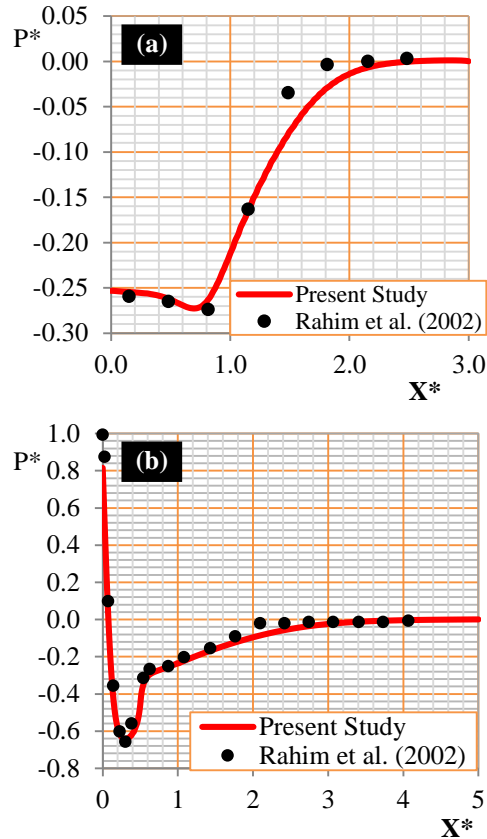
Fig. 4. Comparison of present study with Rahim *et al.* (2002) (a) Variation of P* along casing with X* (b) Variation of P* along liner with X*.

Table 1 Comparison of present study with Rahim *et al.* (2007)

Parameters	Rahim *et al.* (2007)	Present Study	Absolute Error (%)
C$_P$ (%)	27.86	25.37	8.92
λ (%)	68.37	73.08	6.9

3.2. Study on flow field

3.2.1. Study on Streamline Contours

Study on streamline contours is required, to make a qualitative assessment of the change of flow direction and size of the CRZ occurring, during the flow in a dump diffuser. In the present work, a study on streamline contours is required, to analyze the effect of SWA on the nature of GA and CDA variations occurring in the considered model, which govern the size of the CRZ as well as some important performance aspects, which are dealt in the subsequent sections. The streamline contours for some important SWA in the considered range, are presented in Fig. 5. Streamline contours at angles 90°, 30° are shown in Fig. 5(a) and Fig. 5(b)

respectively. It is observed from those figures that the CRZ occurring in both cases is large in both radial and axial directions. The probable reason behind this is that the GA variation occurring in those cases is sharp.
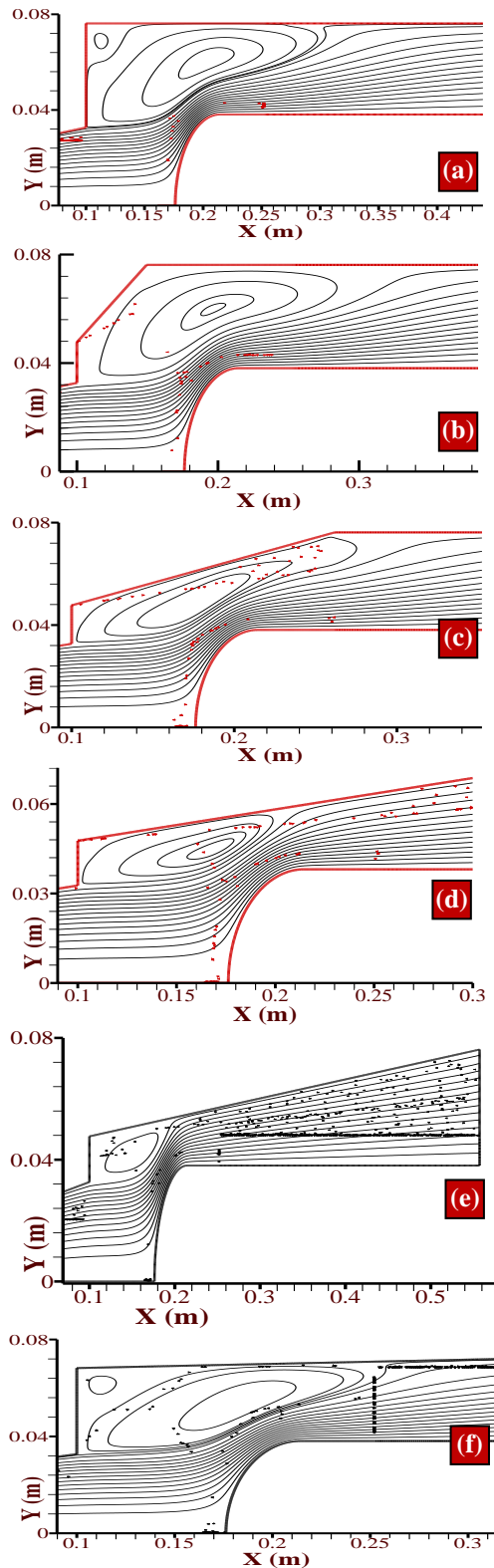
Fig. 5. Streamline contours of flow field at different SWA (a) 90°, (b) 30°, (c) 10°, (d) 6°, (e) 3.57°, (f) 1°.

Streamline contour at SWA 6° is shown in Fig. 5(d). It is noticed that, at this SWA, the radial and axial extensions of the CRZ are much lower. It is because, at such lower SWA, GA variation occurring is more gradual, leading to lower flow reversal and consequently, lesser radial extension of the CRZ. While, the nature of the CDA variation occurring at this angle, is sharper compared to higher angles. This results in earlier flow diffusion into the annular region and consequently lower axial extension of the CRZ. Streamline contour at 3.57° is shown in Fig. 5(e). At this SWA, due to continuous divergence until the outlet, GA variation occurring is too gradual and CDA variation occurring is too sharp. As a consequence, CRZ occurring is observed to be too small, both in radial and axial directions. It is also noticed that the CRZ at this SWA, is almost limited within the dump region only. Streamline contour at SWA of 1° is shown in Fig. 5(f). It is observed that, at this SWA, CRZ is again observed to be large, in both axial and radial directions. It happens because, at this angle, GA variation again becomes sharp and CDA variation is gradual. This results in larger CRZ in both directions.

In this section, qualitative study of the streamline contours for different SWA has been made. From this study, one aspect is noted that there are no considerable changes in the flow pattern, for SWA in the range of between 90° and 11°. But below 11°, significant flow pattern changes have taken place, which has reduced the size of the CRZ in both the directions.

3.2.2   Study on Reattachment Length

Study on the flow reattachment length is required, to have quantitative confirmation of the conclusion regarding the axial extension of the CRZ, which is presented in the preceding section. Figure 6(a) represents the reattachment length considered for any typical case. It is considered to be the distance from the inlet section to the point on the casing wall where the flow reattaches permanently and streamlines become almost horizontal. Figure 6(b) represents the variation of the flow reattachment length on the casing wall, with respect to SWA. It is observed that, at SWA of magnitudes between 90° and 11°, reattachment length is of higher magnitudes. The reason behind this is the larger axial extension of the CRZ, at those higher SWA, as explained in the preceding discussion. It is noticed that reattachment length is almost uninfluenced by the SWA, from 90° to 11°. This observation is in agreement with the conclusion of the preceding section. However, below SWA of 11°, it can be observed that there is a sharp reduction in the reattachment length. This happens because of the sharp reduction in the axial extension of the CRZ, until 3.57°, due to the reason mentioned in the preceding section. Below 3.57°, reattachment length increases again, due to sharp GA variation and consequently larger CRZ occurring at those SWA, as explained earlier.

From the study on reattachment length variation with SWA, it can be reaffirmed that there are no

considerable changes in the flow pattern, for SWA in the range between 90° and 11°. It can also be concluded that the axial extension of the CRZ is larger, at higher magnitudes of SWA.
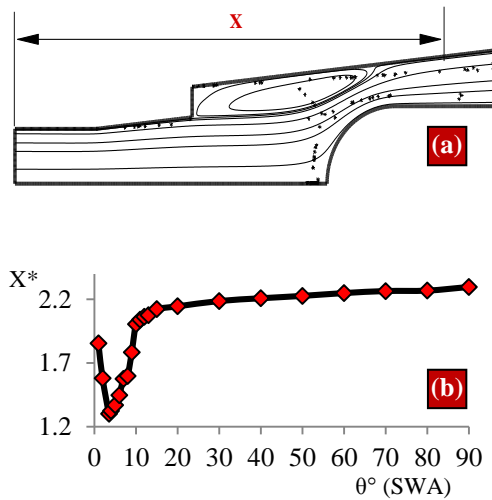
Fig. 6. Study on reattachment length (a) Representation of reattachment length (b) Variation of reattachment length with SWA.

3.2.3   Study on Axial Velocity Profiles

Study of the axial velocity profiles in a dump diffuser is needed, to reveal any interesting flow aspects occurring in the dump and annular regions. In the present section, the effect of considered magnitudes of SWA on the axial velocity profiles has been studied. It is also expected from this study, to provide the information regarding the intensity and radial extension of the CRZ. Figure 7 shows the comparison of the axial velocity profiles for four typical SWA, at five different axial locations. Those five locations are considered in such a way that two locations are in the dump region, two are in the annular region and one is on the dome face. From the outcome of the present study, it is noted that one aspect is common in the profiles, at all the locations, that is, a part of the profile is with negative magnitudes. It is so, as that part of the stream is in the CRZ. The negative magnitudes associated with CRZ are observed to be much lower compared to those of main stream, as the mass trapped in the CRZ is much lower than that of the main flow. Axial velocity profiles at locations $X^*=0.906$, 1.03 are almost similar. It can be observed that at those locations radial height with negative velocity magnitudes is higher, for SWA of 90° and 1°.

This reaffirms the conclusion of preceding sections, that radial extension is comparatively larger for higher SWA (SWA of magnitudes greater than 11°) and for SWA of 1°.

However, negative velocities of CRZ, at SWA of 3.57° and 10° are slightly higher. This is because of relatively sharp CDA variation at those SWA, which causes higher throat velocities and therefore, resulting in higher magnitudes of negative velocity.

From the above observation, it may be concluded that CRZ is more intense at lower SWA than at higher SWA. From axial velocity profile at dome face location, i.e., at $X^*=1.156$, it is observed that main stream velocities have been considerably increased. This happens because, at that location, the flow is in the converging region of the CDA variation. From the velocity profiles at annular locations, i.e., at $X^*= 1.406$, 1.656, it can be observed that the velocity profile of 3.57° is almost stabilized as no negative velocity region is observed. While, at other angles including 1°, 10°, some part of the stream is still observed to be in the recirculation. The reason behind the above observation is the occurrence of relatively smaller CRZ at that SWA. Velocity profile at $X^*=1.656$ is almost similar to that at its previous location. However, for SWA of 90° and 1°, higher main stream velocities are observed at this location. The reason behind this is the occurrence of relatively gradual CDA variation at those SWA. It causes the main stream to still be in the converging region of the CDA variation, which results in higher main stream velocities at that location. It is also observed from the axial velocity profiles at annular locations for SWA of 3.57° that a part of the flow stream is decelerated. This happens because of the contact of that part of the stream with the free surface of the CRZ.

From the study of axial velocity profiles, some significant conclusions can be made. They are as follows. The radial extension of the CRZ is noted to be larger, at higher SWA (SWA between 11° and 90°) as well as at SWA of 1°. The intensity of the CRZ is noted to be higher, at lower SWA (SWA below 11°). Earlier velocity stabilization is noted to occur at SWA of 3.57°.

3.3.   Study on Casing Wall Pressure Variation

Static pressure study along the casing wall is needed to get a qualitative understanding of the static pressure variation along the length of different regions of the dump diffuser. It is expected that the presence of SWA may cause a considerable pressure recovery in the dump and annular regions. This aspect can be realized from the study on the static pressure variation along the casing wall. Along with the above aspect, this study also provides understanding regarding the effect of SWA on the density of the CRZ. Figure 8 shows the variation of P^* along the overall casing wall.

The general trend of pressure variation along the overall casing wall is similar for all the SWA. This general trend can be described as follows. In the initial region of the inlet section, pressure decreases gradually because of the wall friction. After that, it rises sharply in the pre-diffuser section because of solid wall expansion. After pre-diffuser, it remains almost constant at particular magnitude until a certain length because of the presence of the CRZ. This magnitude of static pressure is governed by the density of the CRZ. After that, static pressure increases again at the location, where the main flow reattaches to the casing wall. Finally, it becomes stable after some length in the annular region.
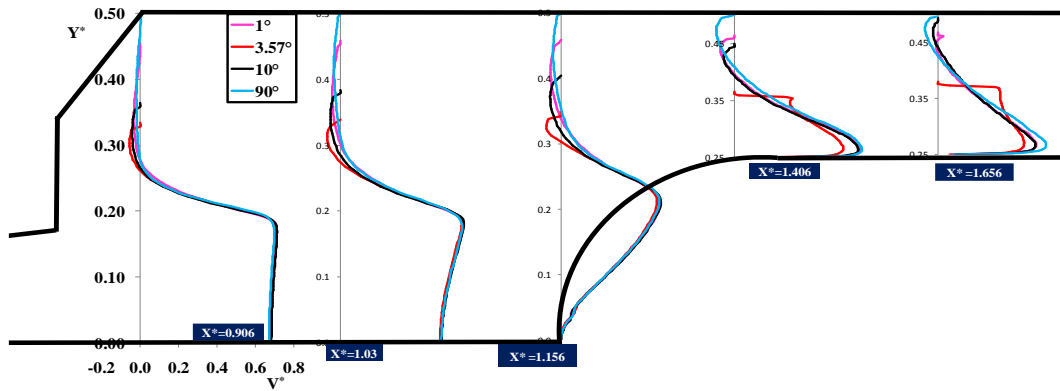
Fig. 7. Comparison of profiles of axial-component of the velocity, at five axial locations, for different SWA.

From Fig. 8, it can be noted that for SWA in the range from 10° to 90°, static pressure variation is similar until the pre-diffuser exit. For those SWA, inlet pressure magnitudes are relatively higher, because of the occurrence of gradual CDA variation. However, for SWA of 3.57° inlet pressure magnitude is comparatively low. This happens because of the occurrence of too sharp CDA variation at that SWA. It can be observed from Fig. 8 that static pressure rise occurring in the pre-diffuser region is almost the same for all the considered SWA.

However, after the pre-diffuser region, noticeable changes are observed in the static pressure variation between the considered SWA magnitudes. It is noted from the study of Fig.8 that at SWA between 10° and 90°, static pressure rise is observed to be very less in the dump and annular regions. But, for SWA of 3.57°, comparatively higher static pressure rise is observed in the dump and annular regions. This happens because of the occurrence of comparatively sharp CDA variation occurring at that SWA. It causes higher magnitudes of free surface diffusion and consequently leading to a relatively higher static pressure rise in the dump and annular regions.

It is also observed from Fig. 8 that, at all the SWA between 30° and 90°, static pressure magnitudes after the pre-diffuser are slightly higher. This is because of higher dense CRZ at those SWA. The probable reason behind the occurrence of higher dense CRZ is the sharp GA variation occurring at those higher SWA. It causes more flow reversal and therefore results in highly dense CRZ. While at 10°, it is observed that, the magnitude of pressure after pre-diffuser is slightly low. This happens because of the gradual GA variation occurring at this SWA. This occurrence results in low dense CRZ at that SWA and therefore causes higher initial pressure magnitudes. It is also observed that pressure stabilization happens comparatively earlier for SWA of 10°. This happens because of the sharp CDA variation occurring at that SWA. It causes earlier flow diffusion and therefore results in earlier pressure stabilization. However, at 3.57°, pre-diffuser exit pressure magnitude is observed to be lower compared to those of the cases with SWA

between 10° and 90°. This is because of the occurrence of more gradual GA variation at that SWA. This occurrence results in low dense CRZ and consequently lower initial pressure magnitude, at that SWA. However, it can be observed from Fig. 8 that static pressure is not at all stabilized along the wall for SWA of 3.57°. This is because of the presence of continuous divergence at that angle. It causes static pressure to increase continuously until the outlet, rather than stabilizing it. This disadvantage at 3.57° may influence the mean pressure magnitudes at the annular region locations.
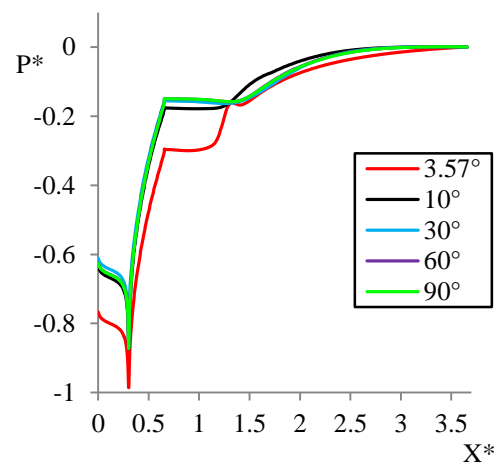
Fig. 8. Comparison of variation of P* along overall casing wall, for different SWA.

However, to study the effect of SWA in a more detailed manner, the present study has been extended to further lower magnitudes of SWA i.e., for SWA of magnitudes less than 10°. Figure 9 shows the static pressure variation along the casing wall in the dump and annular regions, for SWA of magnitudes less than 10°. Static pressure variation in the dump and annular regions is only considered as it is clear from the above discussion that, there is no considerable change in the static pressure variation in the inlet and pre-diffuser regions due to SWA.

It is observed from Fig. 9 that, the magnitudes of initial static pressure decrease gradually with a

decrease in the SWA. This happens because of the occurrence of more gradual GA variation with respect to reduction in the magnitude of SWA. However, in the SWA range between 5° and 8°, it is observed that pressure variation is almost similar. SWA in that range results in early pressure stabilization along with the occurrence of low dense CRZ compared to other higher magnitudes of SWA. This happens because of the reasons that are mentioned earlier. At SWA of 1°, the initial pressure magnitude is observed to be higher compared to that for the SWA between 3.57° and 8°. This happens because of the occurrence of higher dense CRZ occurring at that angle. At that SWA, pressure stabilization is also observed to be delayed. The probable reason behind the delayed stabilization of pressure at that SWA is the occurrence of relatively gradual CDA variation.

From the study of the static pressure variation along the casing wall, one major advantage can be concluded. That is, at lower magnitudes of SWA, there is comparatively higher static pressure recovery in the dump and annular regions. It can also be concluded that lower magnitudes of SWA cause CRZ of low density. It is noted that, among the considered range, SWA of magnitudes between 5° and 8° yields earlier pressure stabilization and low dense CRZ.
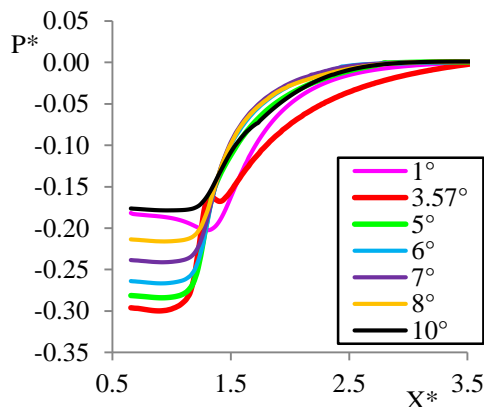
Fig. 9. Comparison of variation of P* along the casing wall (after pre-diffuser), for different SWA below 10°.

3.4. Study on Pressure Variation Along the Liner Wall.

3.4.1. Study on Static Pressure Variation Along the Liner Wall.

Static pressure study along the liner wall is needed, to ensure proper penetration and specified mass flow through the liner holes. It is desirable that the liner wall pressure should become stable as early as possible. It is expected that the presence of SWA can cause effective changes in the pressure distribution along the liner wall. This has motivated the authors to study pressure variation along the liner wall in the present study. Figure 10 shows the comparison of P* variation along the liner wall, for typical SWA. The general trend of pressure variation along the liner wall reaffirms the understanding that is developed regarding the CDA variation in the preceding sections. The reason behind the general trend of pressure variation along the liner wall can be explained as follows. Higher initial pressures are observed at the dome face, as flow becomes stagnant there. Then, it decreases as flow passes through the converging part of CDA variation. After that, it again increases after some length because of divergence in the CDA variation. Finally, it becomes stable after a certain length in the annular region.

It is observed from Fig. 10 that, higher magnitudes of SWA cause higher initial pressure magnitudes at the dome face. It happens because of the higher radial extension of the CRZ, at those SWA. The above-mentioned aspect causes the major part of the main stream to be diverted axially rather than radially. This major part of the stream causes higher magnitudes of pressure when it stagnates at the dome face. However, it is observed from Fig. 10 that pressure stabilization is delayed at SWA greater than 10°. This delay is because of the occurrence of comparatively gradual CDA variation, at those SWA. But at SWA of 10°, slightly earlier stabilization of pressure is observed, because of relatively sharp CDA variation.
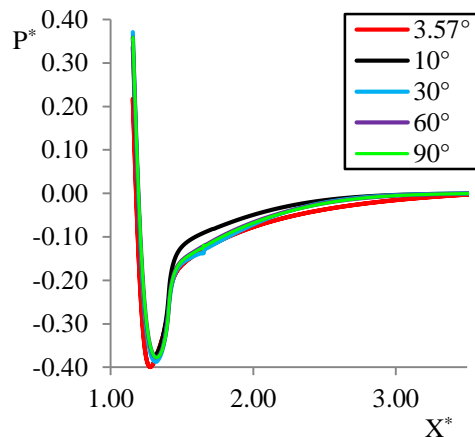
Fig. 10. Comparison of variation of P* with X*, along the liner wall, for different SWA.

However, to study the effect of SWA in a more detailed manner, pressure variation along the liner wall at SWA less than 10° has been studied and presented in Fig. 11. It is observed from both Fig. 10 and Fig. 11 that static pressure is not at all stabilized at 3.57°.

It has remained at lower values at all locations on the liner wall. Though CDA variation is too sharp at that SWA, this happens because of diffusion of the flow into a relatively smaller annular area, which increases continuously until the outlet. This leads to a gradual increase in the static pressure magnitudes until the outlet, without stabilization. While, at SWA between 5° and 90°, the annular area becomes constant at an annular location which changes with the changes in SWA magnitudes. In each case, pressure stabilization takes place at the annular location with respect to the corresponding value of SWA. However, for SWA of magnitudes in the

range between 5° and 10°, earlier stabilization of pressure on the liner wall is observed from Fig. 11. At SWA of magnitude 1°, pressure stabilization is observed to be delayed. This happens because of the occurrence of gradual CDA variation at that SWA.
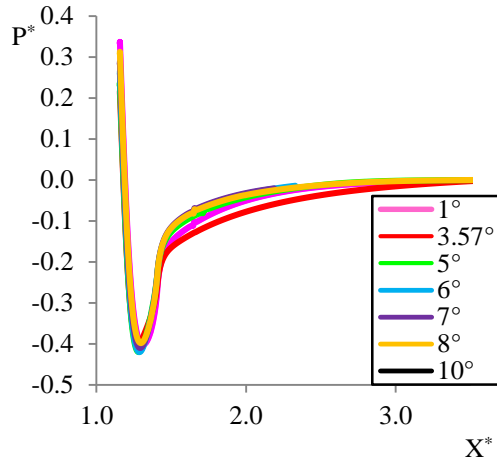
Fig. 11. Comparison of variation of P* along the liner wall, for different SWA below 10°.

From the study of static pressure variation along the liner wall, some significant conclusions may be made. They are as follows. Higher initial pressure magnitudes are observed for magnitudes of SWA between 10° and 90°. Static pressure along the liner wall stabilizes earlier for SWA in the range between 5° and 10°. At SWA of 3.57°, static pressure along the liner wall is not at all stabilized. At SWA of 1°, pressure stabilization is delayed.

3.4.2 Study on Total Pressure Variation Along the Liner Wall

Study on total pressure variation along the liner wall is needed to ensure fluid with higher energy passes through the liner holes. It is desired that total pressure magnitudes along the liner wall should be as high as possible. It is expected that the presence of SWA may cause significant changes in the total pressure distribution along the liner wall. This has motivated the authors to study total pressure variation along an adjacent horizontal line (parallel to the liner wall). This line is considered at a height of 0.002 m above the liner wall. An adjacent line is considered for the study because of the following reason. Along the liner wall, which is under the no-slip condition, the effect of velocity is not manifested in the total pressure magnitudes. It is realized by the authors that there may not be considerable changes in the properties at a height of 0.002 m above the liner wall when compared to those at the liner wall. The above-mentioned height is considered to be acceptable during the study of total pressure variation. Therefore, total pressure variation has been studied along an adjacent line (at a height of 0.002 m).

Equation 6 represents the expression for the mass-weighted mean static pressure. Equation 7 represents the expression for total pressure (P_t).

$$\bar{P} = \frac{1}{\dot{m}} \int_0^A P \, d\dot{m} \tag{6}$$

$$P_t = \bar{P} + \frac{1}{2} \rho V^2 \tag{7}$$

Total pressure has been evaluated as shown in Eq. (7). Fig. 12 represents the comparison of total pressure variation along the considered adjacent line, for different SWA below 10°. The study on total pressure variation for SWA below 10° is only carried out based on the conclusions of the preceding studies that, at SWA of magnitude greater than 10°, pressure stabilization is delayed and also causes higher dense CRZ.
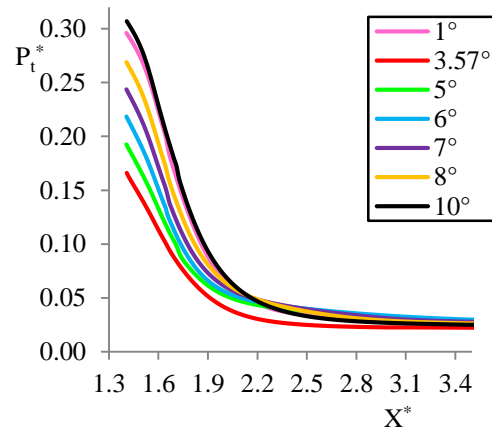
Fig. 12. Comparison of variation of P_t* along a line adjacent to the liner wall, for different SWA below 10°.

Theoretically, for flow without any heat and work transfer, total pressure along the streamline remains constant, when the friction is absent. But, practically total pressure decreases along the streamline because of the presence of friction. The general trend of the total pressure variation in Fig. 12 is of decreasing nature at all SWA. This trend is in agreement with the above mentioned practical conclusion. This general trend may be explained as follows. Initially, total pressure decreases sharply because of losses due to boundary drag caused by the dome wall and free surface of the CRZ. After a certain length i.e., X*=2.2, the decrease in total pressure magnitude is relatively very low as the flow diffuses causing higher values of static pressure.

From Fig. 12, it is observed that before the location indicated by X*=2.2, total pressure magnitudes at a particular location of X* decrease with a decrease in the magnitude of SWA, except those at SWA of 1°. The reason behind this is the occurrence of relatively gradual CDA variation at SWA of 10°, which causes the flow stream to still be in the converging region of CDA variation. But, as the magnitude of SWA decreases below 10°, CDA variation becomes relatively sharp. This cause the flow to be in the diverging region of CDA variation, where it is affected by the free shear stresses. This

occurrence results in a decrease in total pressure magnitudes with respect to decrease in SWA magnitude below 10°. At SWA of 3.57°, total pressure magnitudes are relatively lower because of the reason mentioned in the preceding section.

However, after the location indicated by X^*=2.2, the total pressure magnitudes at all the locations till the outlet are observed to be slightly higher for SWA range between 5° and 10°. It is also observed that total pressure variation is almost similar throughout the considered line, for SWA of magnitudes 1°, 10°. This is because of the occurrence of similar CDA variation at SWA of 1°as that at SWA of 10°.

From the study of total pressure variation along an adjacent line to the liner wall, it is observed that SWA of 3.57° results in comparatively lower magnitudes of total pressure at all the locations along the considered line. It is also observed that SWA of 1° results in similar variation of total pressure as that of SWA of 10°.

3.5.   Study on Static Pressure Recovery and Total Pressure Loss

In any dump diffuser model, the amount of static pressure recovered and total pressure lost are the most important aspects to be evaluated. Study on those aspects is needed to ensure that any modifications made on the dump diffuser model are favorable. It is expected and also concluded qualitatively in the preceding discussions that the presence of SWA can cause higher static pressure recovery in the dump and annular regions. This observation may be quantitatively confirmed by carrying out the quantitative study regarding the overall static pressure recovery and total pressure loss of the dump diffuser. This has motivated the authors to carry out a study on those aspects. Mathematical expressions of static pressure recovery coefficient (C_P) and total pressure loss coefficient (λ) are shown in Eqn. (8) and Eqn. (9) respectively. Static pressure and total pressure terms in Eqn. (8) and Eqn. (9) are evaluated by using Eqn. (6), Eqn. (7) respectively.

$$C_{P1-2} = \frac{\left(\overline{P}_2 - \overline{P}_1 \right)}{0.5\rho U^2} \qquad (8)$$

$$\lambda_{1-2} = \frac{\left(P_{t1} - P_{t2} \right)}{0.5\rho U^2} \qquad (9)$$

These equations are considered from the work of Koutmos *et al.* (1989). Here, subscript 1 indicates the inlet section and subscript 2 indicates the outlet section. $0.5\rho U^2$ is the mathematical expression for inlet dynamic pressure (P_D-IN). Variations of C_P and λ with respect to SWA are shown in Fig. 13 and Fig. 14 respectively. It is observed from Fig. 13 that, in the range of SWA from 11° to 90°, there is no considerable change in the magnitudes of C_P. The reasons behind this occurrence are explained in the earlier discussions. It is also observed that, at those SWA, C_P values are relatively lower, because of the occurrence of the gradual CDA variation. This occurrence causes lower magnitudes of free

surface diffusion, and thereby results in lower magnitudes of C_P. While at SWA below 11°, C_P values are observed to increase sharply with respect to the decrease in the SWA magnitudes till 3.57°. The reason behind this is the occurrence of relatively sharper CDA variation at those SWA, which causes higher magnitudes of free surface diffusion, and thereby results in higher values of C_P. At SWA of magnitudes less than 3.57° i.e., at SWA of 1°, 2°, C_P value is observed to decrease sharply when compared to that at SWA of 3.57°. This happens because of the occurrence of gradual CDA variation at those SWA. It is observed from Fig. 13 that C_P value is found to reach a maximum value of 77.73% at SWA of 3.57°. This happens because of relatively sharper CDA variation occurring at that SWA.
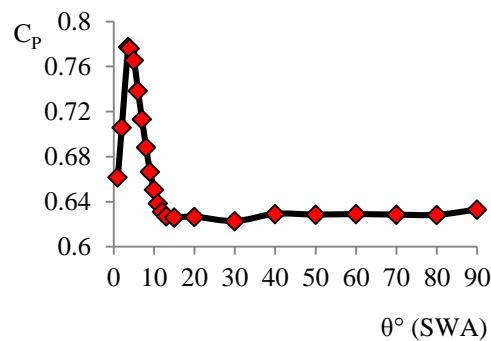
Fig. 13. Variation of static pressure recovery coefficient (C_P) with SWA.
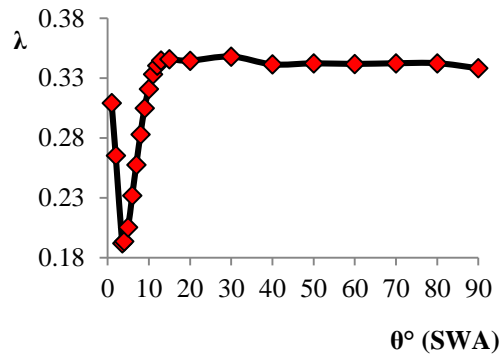
Fig. 14. Variation of total pressure loss coefficient (λ) with SWA.

Table 2 represents the comparison of static pressure recovery and total pressure loss occurring in different sections of the considered dump diffuser model, at typical SWA magnitudes. From Table 2, it is observed that, at all magnitudes of SWA, static pressure recovered within the pre-diffuser section is almost 43.4% to 44% of P_D-IN. However, static pressure recovered in the dump and annular regions is in the range from 24.7% to 33% of P_D-IN, for SWA in the range from 3.57° to 8°. While at SWA from 10° to 90° and at SWA of 1°, that value is in the range between 18% and 22% of P_D-IN. This increase in the static pressure recovery in the dump and annular regions is because of higher magnitudes of free surface diffusion occurring at those SWA.

Table 2 Comparison of static pressure recovery and total pressure loss in different sections of the considered dump diffuser model, at typical SWA

SWA	(P_2-P_1) (% of P_{D-IN})			$(P_{t1}-P_{t2})$ (% of P_{D-IN})		
	Pre-diffuser	Dump and annular regions	Overall diffuser	Pre-diffuser	Dump and annular regions	Overall diffuser
1°	44.45	21.72	66.17	4.02	26.89	30.90
3.57°	44.43	33.31	77.74	4.03	15.17	19.19
5°	44.56	32	76.56	4.24	16.29	20.52
8°	44.13	24.7	68.83	4.13	24.17	28.29
10°	44.13	20.93	65.06	4.13	27.96	32.09
30°	43.43	18.85	62.28	3.87	30.93	34.79
90°	44.33	18.98	63.31	4.19	29.61	33.81

From Fig. 14, it is observed that magnitudes of λ are higher and almost constant for SWA in the range from 11° to 90°. Larger CRZ and gradual diffusion into the annular region cause higher total pressure loss at those SWA. At SWA of magnitudes less than 11°, λ is observed to decrease sharply with the decrease in SWA magnitude until 3.57°.

This happens because of the increase in the magnitudes of static pressure recovered in the dump and annular regions at those SWA. At SWA of magnitudes less than 3.57°, the magnitude of λ is observed to increase. The reasons behind this occurrence are mentioned in the earlier discussions. It is noted that the minimum value of λ of 19.19% occurs at SWA of 3.57°.

From Table 2, it is observed that, at all the magnitudes of SWA, the total pressure loss occurring within the pre-diffuser section is in the range from 3.8% to 4% of P_{D-IN}. However, the total pressure loss in the dump and annular regions is in the range between 15.17% and 24.16% of P_{D-IN}, for SWA in the range between 3.57° and 8°. While at SWA from 10° to 90° and at SWA of 1°, that value is in the range between 26% and 31%.

From the study regarding static pressure recovery and total pressure loss, one major advantage may be concluded. SWA in the range between 3.57° and 8° causes relatively higher static pressure recovery and lower total pressure loss in the dump and annular regions. Static pressure recovery coefficient (C_P) and total pressure loss coefficient (λ) are observed to be maximum and minimum respectively at SWA of 3.57°. Below SWA of 3.57°, performance in terms of static pressure recovery and total pressure loss is observed to degrade.

4. CONCLUDING REMARKS

In the present study, numerical analysis has been carried out on dump diffuser model, to study the effect of sidewall expansion angle on relevant performance aspects and optimize the performance of the model dump diffuser with respect to SWA. Significant conclusions that are made in the present study regarding different aspects of the dump diffuser are summarized below.

- At higher sidewall angles (SWA) i.e., SWA between 10° and 90°, corner recirculation zone (CRZ) observed are highly dense and larger in both radial and axial directions. At those SWA, static pressure stabilization on both casing and liner walls is also delayed.

- There are no considerable changes in terms of any performance aspects, for SWA of magnitudes greater than 11°. This conclusion of the present study is in agreement with that of

  Rhode *et al.* (1983), Sarkar *et al.* (2004), and Kumar *et al.* (2007).

- Presence of lower magnitudes of SWA (SWA less than 10°) results in smaller (radially as well as axially), low dense and higher intense CRZ.

- SWA of magnitude in the range between 5° and 8° is observed to cause earlier pressure stabilization on both the casing and liner walls.

- SWA of magnitudes less than 10° results in comparatively higher static pressure recovery and lower total pressure loss in the dump and annular regions.

- At SWA of 3.57°, Static pressure recovery coefficient (**C_P**) reaches a maximum value of 77.74% and the total pressure loss coefficient (**λ**) reaches a minimum value of 19.19%. At that SWA, earlier velocity stabilization is observed. However, static pressure stabilization on the liner wall is too much delayed and total pressure magnitudes are lower all throughout the liner wall, at that SWA.

- It is observed that, at SWA of magnitudes below 3.57°, performance is found to decline in terms of static pressure recovery and total pressure loss.

Eventually, even though SWA of 3.57° yields a better value of C_P and **λ**. But, it is not optimum magnitude because of disadvantages associated with that SWA. Therefore, the optimum range of magnitude side wall angle (SWA) that may be proposed to yield better performance is between 5° and 7°. This range of SWA yields C_P in the range between 76.55% and 71.32% and **λ** in the range between 20.52% and 25.75%. Along with that aspect, SWA in this range also results in earlier static pressure stabilization and higher magnitudes of total pressure along the liner wall when compared those at SWA of 3.57°.

REFERENCES

Biaglow, J. A. (1971). Effect of Various Diffuser Designs on the Performance of an Experimental Turbojet Combustor Insensitive to Radial Distortion of Inlet Air Flow. *NASA TM* X-2216.

Clarke, D. S., N. S. Wilkes, G. F. Hewitt and S. Jayanti (1990). The Prediction of Turbulent Flows over Roughened Surfaces and Its Application to Interpretation of Mechanisms of Horizontal Annular Flow. Proceedings: Mathematical and Physical Sciences. *The Royal Society* 431(1881), 71-88.

Cohen, H., G. F. C. Rogers, H. I. H. Saravanamuttoo, P. V. Straznicky and A. C. Nix (2017). *Gas Turbine Theory*, Seventh Ed., Pearson education limited, Harlow, UK.

Das, T. and S. Chakrabarti (2015). Flow Characteristics Study in a Configuration of Sudden Expansion with Central Restriction and Fence – Viewed as an Annular Flow Dump Combustor. *Journal of Applied Fluid Mechanics* 8(4), 713-725.

Das, T. and S. Chakrabarti (2016). Pressure Characteristics Study for the Configuration of Sudden Expansion with Central Restriction and Suction. *Open Journal of Fluid Dynamics* 6, 30-41.

Date, A. W. (2005). *Introduction to Computational Fluid Dynamics.* Cambridge University Press, Cambridge, UK.

Fishenden, C. R. and S. J. Stevens (1977). Performance of Annular Combustor-Dump Diffusers. *Journal of Aircraft* 14(1), 60-67.

Ganeshan, V. and R. Thundil Karuppa Raj (2007). Study on the Effect of Various Parameters on Flow Development behind Vane Swirlers. *International Journal of Thermal Sciences* 47, 1204-1225.

Ghose, P., A. Datta and A. Mukhopadhyay (2013). Effect of Dome Shape on Static Pressure Recovery in a Dump Diffuser at Different Inlet Swirl. *International Journal of Emerging Technology and Advanced Engineering* 3(3), 465–471.

Ghose, P., A. Datta and A. Mukhopadhyay (2016). Effect of Prediffuser Angle on the Static Pressure Recovery in Flow through Casing-Liner Annulus of a Gas Turbine Combustor at Various Swirl Levels. *Journal of Thermal Science and Engineering Applications* 8, 011017(1-7).

Gourav, G., S. Bharani, S. N. Singh and V. Seshadri (2002). Effect of Different Annular Heights on the Performance of Annular Gas Turbine Model Combustor. *Indian Journal of Engineering and Materials Sciences* 9, 403-408.

Hestermann, R., S. Kim and S. Wittig (1991). Geometrical Dependence of the Fluid Dynamic Performance Parameters of Plane Combustor Model Diffusers. *Proceedings of Int. Symp. Air Breathing Engines,* 995-1001.

Klein, A. (1995). Characteristics of Combustor Diffusers. *Progress in Aerospace Sciences* 31, 171-271.

Klein, A., K. Katheder and M. Rohlffs (1974). Experimental Investigation of the Performance of Short Annular Combustor-Dump Diffusers. *Proceedings of 2nd Int. Symp. Air Breathing Engines*, University of Sheffield, England, paper no. 23.

Koutmos, P. and J. J. McGuirk (1989). Numerical Calculations of the Flow in Annular Combustor Dump Diffuser Geometries. *Proceedings of the Institution of Mechanical Engineers* 203, 319-331.

Kumar, V. R. S., M. Abhijit, K. Yasir, A. Arokkiaswamy and R. M. O. Gemson (2007). Studies on Dump Diffusers for Modern Aircraft Engines. *AIAA* paper no. 2007-5161.

Lefebvre, A. H. and D. R. Ballal (2010). *Gas Turbine Combustion: Alternative Fuels and Emissions.* 3rd Ed., CRC Press, Boca Raton, FL, 90-92.

Rahim, A., S. N. Singh and S. V. Veeravalli (2007). Liner Dome Shape Effect on the Annulus Flow Characteristics with and without Swirl for a Can-Combustor Model. *Proceedings of the Institution of Mechanical Engineers Part A,* 221, 359–369.

Rahim, A., S. V. Veeravalli and S. N. Singh (2002). Effect of Inlet Swirl and Dump-Gap on the Wall Pressure Distribution of a Model Can-Combustor. *Indian Journal of Engineering and Materials Sciences* 9, 472–479.

Rhode, D. L., D. G. Lilley and D. K. McLaughlin (1983). Mean Flow Fields in Axisymmetric Combustor Geometries with Inlet Swirl. *AIAA Journal* 21(4), 593-600.

Sarkar, A., S. Mondal and A. Datta (2004). Influence of Side Wall Expansion Angle and Swirl Generator on Flow Pattern in a Model Combustor Calculated with K-Ɛ Model. *International Journal of Thermal Sciences* 43, 901-914.

Xia, J. L., G. Yadigaroglu, Y. S. Liu and J. Schmidli (1998). Numerical and Experimental Study of Swirling Flow in a Model Combustor. *International Journal of Heat and Mass Transfer* 41(11), 1485-1497.

Xu, L., Y. Huang, C. Ruan, and P. W. F. Xing (2015). Study of the Dump Diffuser Optimization for Gas Turbine Combustors. *Proceedings of Asia Pacific International Symposium on Aerospace Technology 2014*, Shangai, China, 828 – 834.